

Nov 6th -

# Numerical Simulation on Dynamic Behavior of a Cold-Formed Steel Framing Building Test Model

Yuanqi Li

Rongkui Ma

Zuyan Shen

Follow this and additional works at: <http://scholarsmine.mst.edu/isccss>



Part of the [Structural Engineering Commons](#)

---

## Recommended Citation

Li, Yuanqi; Ma, Rongkui; and Shen, Zuyan, "Numerical Simulation on Dynamic Behavior of a Cold-Formed Steel Framing Building Test Model" (2014). *International Specialty Conference on Cold-Formed Steel Structures*. 2.  
<http://scholarsmine.mst.edu/isccss/22iccfss/session12/2>

This Article - Conference proceedings is brought to you for free and open access by Scholars' Mine. It has been accepted for inclusion in International Specialty Conference on Cold-Formed Steel Structures by an authorized administrator of Scholars' Mine. This work is protected by U. S. Copyright Law. Unauthorized use including reproduction for redistribution requires the permission of the copyright holder. For more information, please contact [scholarsmine@mst.edu](mailto:scholarsmine@mst.edu).

## Numerical Simulation on Dynamic Behavior of a Cold-Formed Steel Framing Building Test Model

Yuanqi Li<sup>1</sup>, Rongkui Ma<sup>2</sup> and Zuyan Shen<sup>3</sup>

### Abstract

A nonlinear dynamic numerical simulation on seismic behavior of a two-story cold-formed steel framing building full-scale shaking table test model was carried out by the way of from components to integral structure. Firstly, refined numerical model of shear wall was established, and restoring force models of screw connections between the framing and sheathings were integrated into the numerical model of shear wall. The refined numerical model of shear wall was verified by tests. Secondly, based on refined numerical model of shear wall and modified exponential "Foschi" skeleton curve, uniform restoring force skeleton curves of two typical shear walls of the shaking table test model were obtained. Then, a simplified numerical model of shear wall was proposed. Finally, a dynamic numerical model of cold-formed steel framing building was established based on the simplified shear wall model and assumption of rigid diaphragm, and nonlinear dynamic analysis was carried out. The results of numerical simulation agreed well with the tests, which indicated that the numerical model of integral buildings can factually reflect the dynamic behavior of cold-formed steel framing building.

### Introduction

Cold-formed steel (CFS) framing system came from North America and Australia. Because of some advantages, such as high construction efficiency, good environment protection and seismic performance, CFS framing system has appeared universally in China in recent years. In order to study the seismic behavior of CFS framing system and verify the application to the seismic fortification area in China, a series of shaking table tests of integral structures (Huang et al. 2011; Li et al. 2012a; Li et al. 2013) were carried out. However, due to the limitations of tests, experimental study is only applied to structures which had certain arrangements. And, the existing studies on nonlinear dynamic behavior of

---

<sup>1</sup> Professor, Department of Building Engineering, Tongji University, State Key Laboratory of Disaster Reduction in Civil Engineering, Shanghai 200092, China. E-mail: liyq@tongji.edu.cn

<sup>2</sup> Doctoral student, Department of Building Engineering, Tongji University, Shanghai 200092, China.

<sup>3</sup> Professor, Department of Building Engineering, Tongji University, State Key Laboratory of Disaster Reduction in Civil Engineering, Shanghai 200092, China.

CFS framing system were not enough to understand the seismic performance of this type of structures. In contrast, there were relatively systemic studies on seismic behavior of light-wood framing structures, especially on the field of numerical simulation. The CFS framing system has similar structure arrangements to light-wood framing structures. However, there are some differences for these two types of structures, such as the connectors and framing materials et al.

A nonlinear dynamic numerical simulation on seismic behavior of a two-story cold-formed steel framing building full-scale test model was carried out by the way of from components to integral structure. Firstly, refined numerical model of shear wall was established based on the restoring force characteristic of screw connections between the studs and sheathings. And the refined numerical model of shear wall was verified by tests. Secondly, based on refined numerical model of shear wall and modified exponential “Foschi” skeleton curve, uniform restoring force skeleton curves of two typical shear walls (sheathed with OSBs + PGBs (papered gypsum boards), and PGBs at double sides) of the shaking table test model were obtained. Then, a simplified numerical model of shear walls was proposed. Finally, a dynamic numerical model of a cold-formed steel framing building test model was established based on the simplified shear wall model and assumption of rigid diaphragm, and nonlinear dynamic analysis was carried out and compared with the tests.

### **Brief introduction of shaking table tests**

The shaking table test model of cold-formed steel framing building simulated in this paper was cited in the reference by Li et al. (2012a). As shown in Fig. 1, the model contained two floors, and was made in full scale. The plan is shown in Fig. 2. The plan size of first floor is 4×6 m, and the plan size of second floor is 4×5.4 m. The height of the first floor is 3.0m, the second floor is 2.8m, and the total height to top of roof is 6.915 m. The shear walls of the model have sheathings at double sides. The exterior shear walls have OSBs sheathed at outer side and papered gypsum boards sheathed at inner side. The interior shear wall has papered gypsum boards sheathed at both sides. As shown in Fig. 2, No. 1 and 4 are continuous shear walls with no openings, No. 6, 7 and 11 are shear walls with door openings having the size of 1.2×1.2 m, and No. 2, 3, 5, 8, 9 and 10 are shear walls with window openings having the size of 0.9×2.1 m.

Three actual seismic wave records, including El. centro, Qianan and Beijing, and one Shanghai artificial wave were used in the shaking table tests. Three kinds of earthquake intensity were included, such as basic intensity, intensity of frequently occurred earthquake and intensity of seldom occurred earthquake. Tests were carried out according to the rule that the acceleration increased gradually from 0.035 g to 0.1 g, 0.22 g, 0.4 g and 0.62 g, respectively.



Fig. 1. Shaking table test model

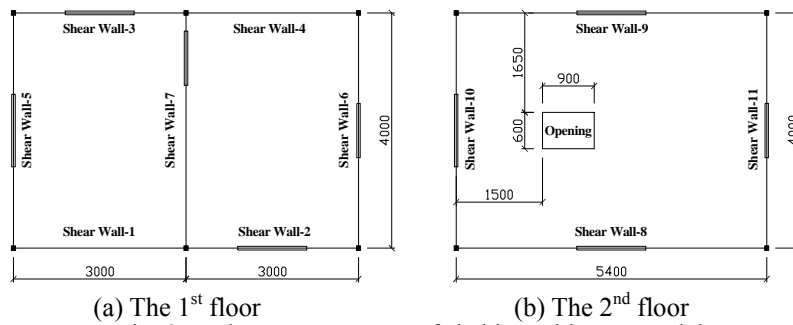
(a) The 1<sup>st</sup> floor(b) The 2<sup>nd</sup> floor

Fig. 2. Plan arrangements of shaking table test model

### Refined numerical model of shear wall

#### *Brief introduction of shear wall test specimens*

The shear walls simulated in this section was cited in the reference by Li et al. (2012b). Twelve shear walls, sheathed with OSBs + PGBs (papered gypsum boards) and steel sheathings + PGBs, respectively, were designed and tested in monotonic and cyclic loading modes, respectively. The details of specimens are summarized in Table 1.

Table 1. The details of tested shear walls

Specimen	Construction	Opening size (m×m)	Loading mode
SW1		-	monotonic
SW2		-	monotonic
SW3	width ×height: 2.4×3.0 m;	-	cyclic
SW4	sheathings: 12 mm OSBs	0.6×1.2	monotonic
SW5	+ 12 mm PGBs	0.6×1.2	monotonic
SW6		0.6×1.2	cyclic

SW7		1.2×1.2	cyclic
SW8		1.2×2.1 (in the middle)	cyclic
SW9		1.2×2.1 (at the side)	cyclic
SW10	width×height: 2.4×3.0 m;	-	monotonic
SW11	sheathings: 12 mm PGBs	-	cyclic
SW12	+ 0.5 mm steel sheathings	0.6×1.2	cyclic

The studs with the thickness 0.8 mm and nominal yield strength 345MPa were used to comprise the framing. And the space of the studs is 600mm. Two kinds of sheathings were used, including OSBs and PGBs. Sheathings were connected to the framing by screws with the spacing of 150 mm in borderline and 300mm inside. The hold-down devices were set at the ends of the side studs with M16 bolts.

#### **Refined numerical model of shear wall**

For shear walls simulated in this paper, the framing studs were modeled as 3D elastic frame elements in order to take into account that these elements were not heavily deformed in the post-elastic range. The top girder was fastened firmly to rigid loading beam, and the bottom girder was fastened firmly to rigid support. So, the top and bottom girders were considered as the rigid members by means of increasing their elastic modulus.

As the framing deforms into a parallelogram, the OSBs and PGBs have rigid-body rotation. The OSBs have the larger shear stiffness in plane than the framing, and mainly have the deformation of rigid torsion in the horizontal loading. So, the OSBs were modeled as isotropic elastic shell elements when loaded in shear. The elastic modulus and Poisson's ratio were valued as 3500 MPa (National Technical Committee 198 2010) and 0.3 (Thomas 2002), respectively. And PGBs were also modeled as isotropic elastic shell elements. The elastic modulus and Poisson's ratio were valued as 1587 MPa and 0.23 (Kasal et al. 1992), respectively.

Connections among the framing members were modeled as hinges. And, connections between the studs and sheathings were modeled using two-freedom spring elements in order to taking into account that the spring elements were used to simulate the average deformation properties along and perpendicular to the loading directions. The modified exponential “Foschi” skeleton curve was used to simulate the behavior of stud-sheathing screw connections in shear loading.

The modified exponential “Foschi” curve (Dolan 1989; Folz et al. 2001) is characterized by formula (1) which contains 6 parameters,  $k_1$ ,  $k_2$ ,  $k_3$ ,  $F_0$ ,  $\delta_m$  and  $\delta_u$ , respectively. Where  $k_1$  is the initial stiffness,  $k_2$  is the slope of the asymptotic line of the exponential curve,  $k_3$  is the slope of the linear decreasing section,  $F_0$  is the initial load,  $\delta_m$  is the deformation at peak load, and  $\delta_u$  is the ultimate deformation.

$$F = \begin{cases} \operatorname{sgn}(\delta) \cdot (F_0 + K_2 |\delta|) (1 - e^{-\frac{K_1 |\delta|}{F_0}}), & |\delta| \leq \delta_m \\ \operatorname{sgn}(\delta) \cdot F_m + K_3 (\delta - \operatorname{sgn}(\delta) \cdot \delta_m), & \delta_m < |\delta| \leq \delta_u \\ 0, & |\delta| > \delta_u \end{cases} \quad (1)$$

Table 2. Parameters of modified exponential “Foschi” skeleton curve

Type of connections	$k_1$ (kN/mm)	$k_2$ (kN/mm)	$k_3$ (kN/mm)	$F_0$ (kN)	$\delta_m$ (mm)	$\delta_u$ (mm)
Stud-OSB	1.869	0.098	-0.125	1.224	6.6	18.6
Stud-PGB	1.200	0.029	-0.016	0.319	4.5	27.0
Stud-steel sheathing	1.438	0.230	-0.272	1.368	6.4	12.9

The parameters of cold-formed steel stud-sheathing connections advanced by Ma (2014) are summarized in Table 2, where the thicknesses of studs, OSBs, PGBs and steel sheathings are 0.8, 12, 12, 0.5 mm, respectively. The ultimate deformation  $\delta_u$  of the first two connections was valued as the deformation corresponding to  $0.2F_m$  on the post-peak branch of response, and  $\delta_u$  of stud-sheathing connection was valued as the deformation corresponding to  $0.5F_m$  on the post-peak branch of response.

#### ***Verification of refined numerical model***

Refined numerical model was established by structural analysis program SAP2000 to reproduce the behavior of the entire shear wall. The numerical model was subjected to increasing horizontal deformation at the upper part of the shear wall model, which was consistent with shear walls during the tests. The evaluated results, including deformed shape and the load vs. deformation curves, were compared with the tests.

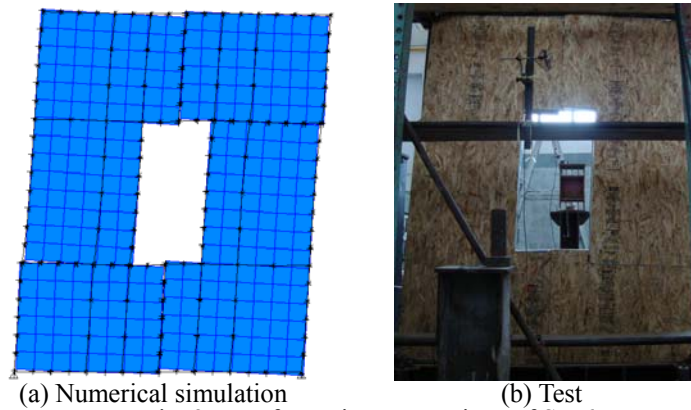


Fig. 3. Deformation comparison of SW6

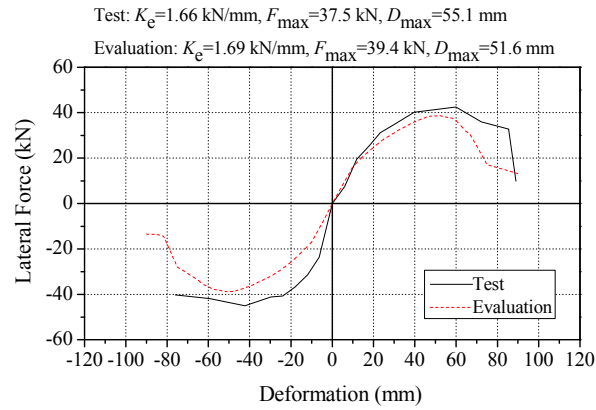


Fig. 4. Load vs. deformation curve comparison of SW11

Fig. 3 presents the deformation comparison between the evaluation and test for specimen SW6. As shown in Fig. 3, the remarkable similarities of deformed shape can be seen.

Fig. 4 presents the comparison of load vs. deformation curves between the evaluation and test for specimen SW11. As shown in Fig. 4, the load vs. deformation skeleton curves of the evaluation agree well with the tests, and evaluation of the characteristic parameters including  $K_e$ ,  $F_{max}$  and  $D_{max}$ , was close to the tests, which indicates that the performance of shear walls can be accurately evaluated through the numerical simulation technique.

#### ***Uniform restoring force skeleton curves of shear walls***

Because of having a large number of elements, the refined shear wall model is not suitable to be integrated into the numerical model of integral building. By contrast, the equivalent bracing model has an obvious advantage of high efficiency because of the brief conformation. However, the restoring force characteristic of bracing depends on testing, which is the problem that the equivalent bracing model is not directly used to evaluate the performance of shear walls. So, if the restoring force characteristic of shear wall (or bracing) was obtained, the problem stated above was easily resolved.

There are two types of shear walls in the shaking table test model, including the exterior shear walls sheathed with OSBs and PGBs at each side, and the interior shear wall sheathed with PGBs at both sides. In order to obtain the skeleton curves of the two types of shear walls contained in shaking table test model, refined numerical models without openings of the two types of shear walls were established, and the relationship of load vs. deformation was obtained through numerical simulation. Then, the uniform skeleton curves for a unit width of the two types of shear walls were characterized by the modified exponential ‘‘Foschi’’ skeleton curve which was formulized as the formula (1). According to Chinese specification JGJ 101 (1997), the ultimate deformation  $\delta_u$  was valued as the deformation corresponding to 0.85 $F_m$  on the post-peak branch of response.

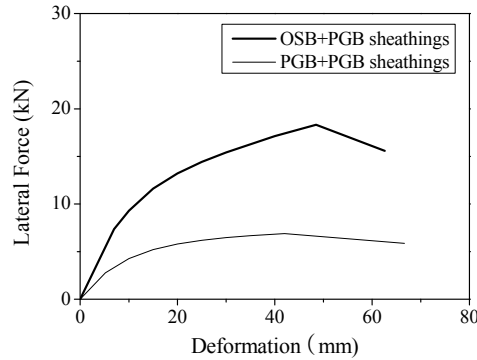


Fig. 5. Uniform skeleton curves of two typical shear walls for a unit width

Table 3. Parameters of uniform exponential “Foschi” skeleton curve

Type of shear wall	$k_1$ (kN/mm)	$k_2$ (kN/mm)	$k_3$ (kN/mm)	$F_0$ (kN)	$\delta_m$ (mm)	$\delta_u$ (mm)
OSB+PGB	1.467	0.142	-0.195	11.510	48.5	62.6
PGB+PGB	0.695	0.023	-0.042	5.988	42.0	66.6

The two typical uniform skeleton curves obtained by the modified exponential “Foschi” skeleton curve were shown in Fig. 5, and the corresponding parameters were summarized in Table 3. So, the load vs. deformation relationship of the two typical shear walls with different widths can be easily obtained through the uniform skeleton curves. For shear walls with openings, only the sections without openings were considered in resisting the lateral force, and the contribution of the opening section can be ignored. According to the principle, it is simple enough to produce the behavior of shear walls by the numerical technique. And, the uniform skeleton curves can also be used in the numerical model of integral buildings.

## Numerical model of integral building

### *Simplified numerical model of shear wall*

The diaphragm effect generated by the sheathings is modeled by equivalent nonlinear bracing which can bear the axial force along its axis. The framing is modeled by four rigid members along the outer contour of shear walls, and the rigid members are considered to be pinned. The mass of shear wall is equally distributed to the upper parts of columns. The simplified numerical model of shear wall is shown in Fig. 6.

The stiffness and strength of shear wall are provided by the equivalent nonlinear bracing, and the sideway is depended on deformation of the frame and bracing. The relationship of load vs. deformation of the equivalent nonlinear bracing can be obtained from Fig. 8, as is shown in formulas (2) ~ (4), where  $D$ ,  $K$  and  $F$  define the sideway, lateral stiffness and strength of shear wall, respectively, and  $D'$ ,  $K'$  and  $F'$  define the axial deformation, stiffness and strength of bracing, respectively.

$$D' = D \cdot \cos \theta \quad (2)$$



$$F' = \frac{F}{\cos \theta} \quad (3)$$

$$K' = \frac{F'}{D'} = K \cdot \frac{1}{\cos^2 \theta} \quad (4)$$

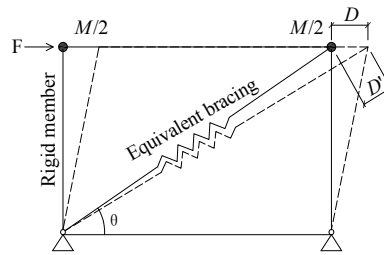


Fig. 6. Simplified shear wall model

#### **Numerical model of cross steel strips**

The cross steel strips bear the axial tension as the shear wall bears the lateral force, which can greatly improve the shear behavior of shear walls. It was found that tensile fracture occurred in net section of cross steel strips during the shaking table tests, as is indicated that the cross strips reached the ultimate state. So, the axial plastic hinges were considered to evaluate the behavior of cross steel strips. The relationship of load vs. deformation of axial plastic hinge is shown in Fig. 7. Where “A” means the zero stress state, “B” means the hinge reaches the yield state, “C” means the hinge reaches the ultimate state, “D” means the hinge reaches the post ultimate state, and “E” means the fracture of cross strips.

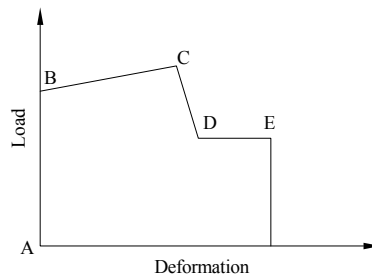


Fig. 7. Plastic hinge model of steel strips

#### **Numerical model of floor and roof**

The floor of shaking table test model was composed of framing beams, lateral braces, sheathings and a layer of plain concrete. So, the floor has the much larger shear stiffness compared with the shear walls. So, rigid diaphragm assumption was adopted to model the floor. For roof system, the rigid diaphragm assumption was also adopted.

#### **The mass of shaking table test model**

The live load of a residential building floor is valued as 2.0 kN/m<sup>2</sup>

according to Chinese specification GB50009 (2006). When earthquake action is considered, the combination coefficient of the floor live load is valued as 0.5 in calculating representative value of gravity load according to Chinese specification GB50011(2001). So the additional mass put on the floor slab is about 100 kg/m<sup>2</sup>. And the total mass of the floor has been evaluated to about 2985 kg added the self-weight of the floor. The total mass of the roof has been evaluated to about 260 kg.

The exterior shear walls were sheathed with OSBs (added calcium silicate boards) and PGBs at each side with the mean areal density about 40 kg/m<sup>2</sup>. The interior shear wall was sheathed with PGBs at both sides with the mean areal density about 25 kg/m<sup>2</sup>. The total mass of walls of the first floor is about 2180 kg which was uniformly distributed to the six mass points at the height of 3.0 m. The total mass of walls of the second floor is about 1678 kg which was uniformly distributed to the four mass points at the height of 5.8 m.

#### ***Vibration modes and periods***

The first three vibration modes of the integral structure have been evaluated using the structural analysis program SAP2000 and the periods of vibration were obtained. As shown in Fig. 8, translational motions in Y and X axis were the first two vibration modes accompanied by slight retortion, and retortion around Z axis was the third vibration modes. Table 4 summarizes the first three periods of vibrations obtained by the tests and numerical evaluation. It is indicated from Table 4 that the periods obtained by numerical evaluation agreed well with the tests.

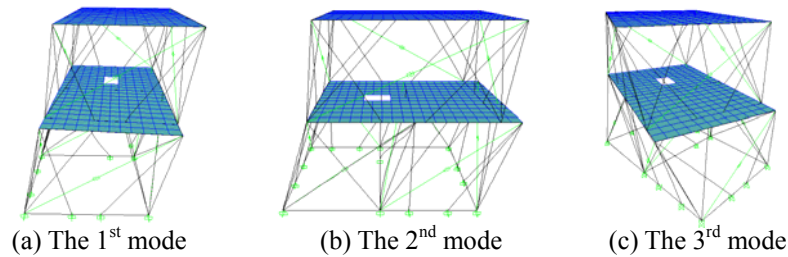


Fig. 8. First three vibration modes

Table 4. Vibration periods comparisons of evaluations and tests

Vibration mode	Tests (Li et al. 2012a) (s)	Simulation (s)
UY	0.147	0.149
UX	0.130	0.132
RotZ	0.106	0.113

### **Nonlinear dynamic analysis of integral building**

#### ***Damping ratio and Railgh damping coefficient***

Railygh damping principle was integrated into the numerical model to produce the dynamic response of integral structure. Railygh damping principle is expressed by formulas (5) ~ (7) (Clough et al. 2006).

$$c = a_0 M + a_1 K \quad (5)$$

$$a_0 = \frac{2\xi\omega_m\omega_n}{\omega_m + \omega_n} \quad (6)$$

$$a_1 = \frac{2\xi}{\omega_m + \omega_n} \quad (7)$$

where  $c$  is the Railgh damping coefficient,  $a_0$  presents the damping coefficient of quality,  $a_1$  presents the damping coefficient of stiffness,  $M$  presents the mass matrix,  $K$  presents the stiffness matrix,  $\xi$  presents the damping ratio, and  $\omega_m$  and  $\omega_n$  present the  $m^{\text{th}}$  and  $n^{\text{th}}$  circular frequencies, respectively.

The shaking table test model has a regular structural arrangement and uniform distribution of mass and stiffness, and translational motions in  $Y$  and  $X$  axis were the first two vibration modes. So, the first two circular frequencies  $\omega_1$  and  $\omega_2$  were taken.

The damping ratios of the shaking table test model simulated in this paper were obtained through scanning frequency by white noise when loading cases for different earthquake intensity were finished. In frequently occurred earthquake, the damping ratio was measured as about 0.03. And in rarely occurred earthquake, the damping ratio was in the range of 0.03 ~ 0.07. Yet, after the 1st loading case of 0.62 g series, the damping ratio was measured as 0.052.

According to the above studies, the damping ratios of the integral model simulated in this paper were taken as: 0.03 for 0.035 g and 0.1 g series, 0.04 for 0.22 g series, and 0.05 for 0.4 g and 0.62 g series.

### **Results of numerical evaluation**

The numerical model was subjected to a series of seismic loadings which were consistent with the tests. Direct integration method was adopted to perform the responses of the integral building, and results obtained with the numerical model were compared with the tests.

Fig. 9 summarizes the acceleration comparisons of numerical evaluation and tests. Where the loading cases T2~T9 were included in 0.035 g series, T11~T18 were included in 0.1 g series, T20~T27 were included in 0.22 g series, T29~T36 were included in 0.4 g series, and T38~T45 were included in 0.62 g series. In order to verify the numerical model, the measured points of numerical model were consistent with the tests. For the loading cases of 0.035 g and 0.1 g series, the deviation of numerical evaluation was in the range of -39.3%~46.8%. However, the absolute value was smaller compared to the tests. For the 0.22 g series, the deviation of numerical evaluation was in the range of -30.2%~47.2%. For the 0.4 g series, the deviation of numerical evaluation was in the range of -17.4%~23.4%. And for the 0.62 g series, the deviation of numerical evaluation was in the range of -21.0%~20.3%. Overall, the evaluations in 0.035, 0.1 and 0.22 g series had slightly larger accelerations compared with the tests, and evaluations in 0.4 g series had equivalent accelerations with the tests. When loading case increased to 0.62 g, the evaluations were slightly smaller than the tests.

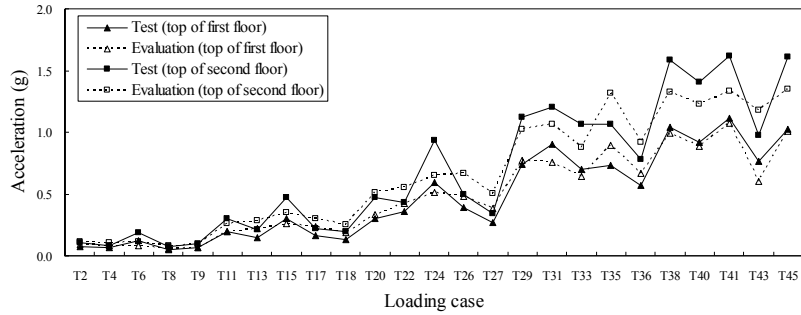


Fig. 9. Comparisons of maximum acceleration

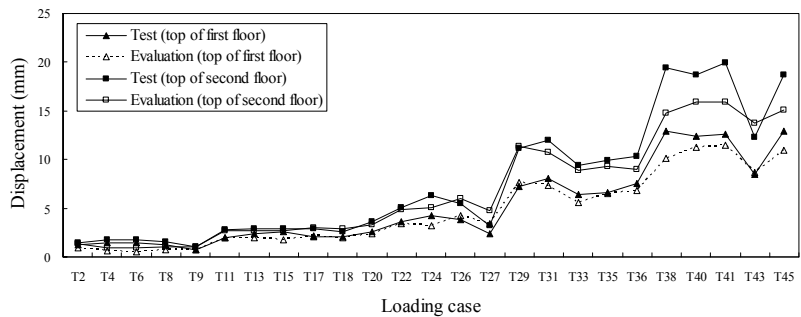


Fig. 10. Comparisons of maximum displacement

Fig. 10 summarizes the relative displacement comparisons of numerical evaluation and tests. As shown in Fig. 10, the evaluations agreed well with the tests in the case of T2~T29 corresponding to 0.035 g~0.22 g series. And when the seismic action increased to 0.4 g and 0.62 g, the evaluations were getting smaller than the tests.

There had been accumulated damage in the test model during a series of the increasing seismic action, which resulted in decrease of the structural stiffness and increase of the structural response. Yet, the accumulated damage was not included in numerical model. So, the numerical evaluation was getting smaller than the tests when the seismic action increased.

#### **Results of time-history of acceleration and displacement**

The time-histories of acceleration and displacement of integral model were evaluated by SAP2000 and were compared with the tests. Fig. 11 presents the acceleration time-history comparison in  $X$  direction in the case of T38 loading case (0.62 g). It can be seen from Fig. 11 that the figure of evaluation were consistent with the test, and the evaluated maximum acceleration at the top of 2<sup>nd</sup> floor was 1.325 g, with the deviation of -16.4%. Fig. 12 also presents the displacement time-history comparison in  $X$  direction in the case of T38 loading case (0.62 g). It can be seen from Fig. 12 that the figure of evaluation was roughly consistent with the tests, and the evaluated maximum displacement at the top of 2<sup>nd</sup> floor was 12.93 mm, with the deviation of -12.0%.

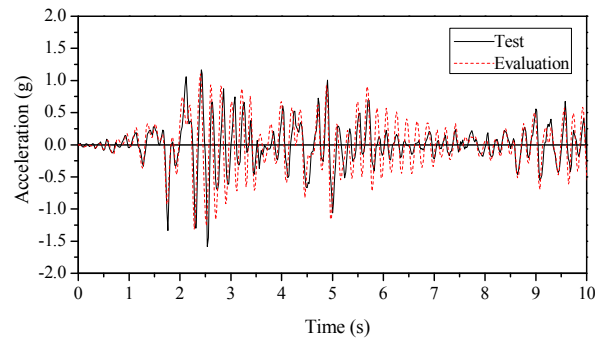


Fig. 11. Acceleration time-history comparisons

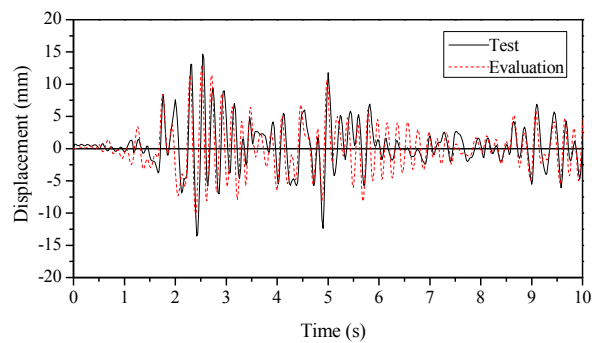


Fig. 12. Displacement time-history comparisons

## Conclusions

A refined numerical model of shear wall was established based on the restoring force models of screw connections between the framing and sheathings. A numerical analysis was carried out, and the numerical results agreed well with the tests, which indicated that the numerical shear wall model can accurately reflect the seismic behavior of shear walls.

Based on refined numerical shear wall model and modified exponential “Foschi” skeleton curve, uniform restoring force skeleton curves of two typical shear walls (sheathed with OSBs + PGBs, and PGBs at both sides) were proposed. And, the uniform skeleton curves can be integrated into the simplified numerical shear wall or integral building models, which would greatly improve the efficiency of the numerical simulation.

A dynamic numerical model of a two-story cold-formed steel framing building full-scale test model was established based on the simplified shear wall model and assumption of rigid diaphragm, and nonlinear dynamic analysis was carried out. The results of numerical simulation agreed well with the tests, and the numerical model can factually reflect the seismic behavior of integral buildings.

## Acknowledgements

Authors are grateful to the financial support by the National Natural

Science Foundation of China (No.50878168) and the 12th National Five-Year Science and Technology Support Project (No.2012BAJ13B02).

## References

- Clough, R., Penzien, J. (Wang, G. et al. Translation.) (2006). *Dynamics of Structures Edition Two (Revised Edition)*. Higher Education Press, Beijing, China.
- Dolan, J. D. (1989). "The Dynamic Response of Timber Shear Walls." Department of Civil Engineering, University of British Columbia, Vancouver, B.C, Canada.
- Folz, B., Filiatrault, A. (2001). "Cyclic Analysis of Wood Shear Walls." *Journal of Structural Engineering*, 127(4): 433-441.
- Huang, Z., Su M., He B., Shen L., Qi Y., Sun J., Yu F. (2011). "Shaking Table Test on Seismic Behaviors of Three-Story Cold-Formed Thin-Wall Steel Residential Buildings." *China Civil Engineering Journal*, 44(2): 72-81.
- JGJ 101-96. (1997). "Specification of Testing Methods for Earthquake Resistant Building." China Architecture and Building Press, Beijing, China.
- Kasal, B., Leichti, R. J. (1992). "Nonlinear Finite Element Model for Light-Frame Stud Walls." *Journal of Structural Engineering*, 118(11): 3122-3135.
- Li, Y., Liu, F., Shen, Z., He, H. (2012a). "Shaking Table Test of Two Full-Scale Models of S350 Cold-Formed Thin-Walled Steel Framing Buildings." *China Civil Engineering Journal*, 45(10): 135-144.
- Li, Y., Liu, F., Shen, Z., He, H. (2012b). "Experimental Investigation on Seismic Behavior of S350 Light-Gauge Composite Framing Walls." *China Civil Engineering Journal*, 45(12): 83-90.
- Li, Y., Liu, F., Shen, Z., Shen, L., Qin, Y. (2013). "Shaking Table Test on a Full-Scale Models of Low-Rise High-Strength Cold-Formed Thin-Walled Steel Framing Buildings." *Journal of Building Structures*, 34(1): 36-43.
- Ma, R. (2014). "Refined Numerical Simulation on Seismic Behavior of Low-Rise Cold-Formed Thin-Walled Steel Framing Buildings." Tongji University, Shanghai, China.
- Ministry of Construction of China. (2006). "GB50009-2001 Load Code for the Design of Building Structures. 2006 Edition." China Architecture and Building Press, Beijing, China.
- Ministry of Housing and Urban-Rural Development of China. (2001). "GB50011-2001 Code for Seismic Design of Buildings." China Architecture and Building Press, Beijing, China.
- National Technical Committee 198 on Wood-based Panels of Standardization Administration of China. (2010). "LY/T 1580-2010 Oriented Strand Board." Beijing: China Standard Press.
- Thomas, W. H. (2002). "Concentrated Load Capacity and Stiffness of Oriented Strand Board: Calculation versus Test." *Journal of Structural Engineering*, 128(7): 908-912.